ISSN 1063-7834, Physics of the Solid State, 2013, Vol. 55, No. 12, pp. 2422–2430. © Pleiades Publishing, Ltd., 2013.
Original Russian Text © D.A. Balaev, S.V. Semenov, M.I. Petrov, 2013, published in Fizika Tverdogo Tela, 2013, Vol. 55, No. 12, pp. 2305–2312.

SUPERCONDUCTIVITY

Dominant Influence of the Compression Effect of a Magnetic Flux in the Intergranular Medium of a Granular High-Temperature Superconductor on Dissipation Processes in an External Magnetic Field

D. A. Balaev, S. V. Semenov, and M. I. Petrov

Kirensky Institute of Physics, Siberian Branch of the Russian Academy of Sciences, Akademgorodok 50–38, Krasnoyarsk, 660036 Russia

e-mail: smp@iph.krasn.ru

Received April 16, 2013

Abstract—Experiments have been presented that demonstrate the effect of the compression of a magnetic flux in grain boundaries of a granular high-temperature superconductor in an external magnetic field on the dissipation processes. The compression of the magnetic flux is associated with the diamagnetic behavior of superconducting grains and the existence of a Josephson medium in grain boundaries. Under these conditions, grain boundaries are in an effective magnetic field that depends on the magnetic state (magnetization) of the superconducting grains. Based on the analysis of experimental data (dependences of the electrical resistance R and magnetization on the magnetic field H and temperature T, as well as current–voltage characteristics), the conclusion has been drawn that it is the temperature evolution of the effective magnetic field in the intergranular medium which primarily determines the behavior of the dependences $R(T)$ in weak external magnetic fields of no more than ~10^3 Oe. This should be taken into account in the interpretation of experiments on the magnetoresistance effect in granular high-temperature superconductors in terms of different theories. The conclusion drawn here also implies a significant correction of the previously obtained results.

DOI: 10.1134/S1063783413120044

1. INTRODUCTION

Granular high-temperature superconductors (HTSCs) in relation to the transport and magnetic properties can be considered as a "two-phase" system. Superconducting grains make a dominant contribution to the magnetic properties (magnetization hysteresis loop, levitating ability of the material) of these objects in magnetic fields from a few oersteds and higher. However, the transport properties are mainly limited to that the superconducting current inevitably flows through the second subsystem, i.e., grain boundaries. The smallness of the geometric length of grain boundaries (on the order of nanometers) makes possible the existence of a weak Josephson coupling between the HTSC grains. On the one hand, the existence of grain boundaries significantly decreases the critical current density of bulk HTSC materials as compared to single crystals, but, on the other hand, it provides the possibility of investigating the processes of superconducting current flow and dissipation in the so-called Josephson medium [1] consisting of superconducting grains and grain boundaries. It should be noted that the magnetic response of the Josephson medium, i.e., the magnetization hysteresis that is characteristic of type II superconductors, manifests itself in magnetic fields of the order of several oersteds at low temperatures ($T/T_c \sim 0.05$, where T_c is the critical temperature) and in magnetic fields of the order of the Earth's field and lower in the vicinity of T_c [2, 3] (at $T/T_c \sim 0.7$–0.8, which corresponds to the range near the boiling temperature of liquid nitrogen).

The existence of the Josephson medium in a bulk material has attracted the particular attention of researchers after the discovery of high-temperature superconductivity. The resistive transition in a granular HTSC reflects contributions from two subsystems: (i) the contribution from HTSC grains, which corresponds to a sharp decrease in the electrical resistance and a very weak influence of external magnetic fields up to ~10^3 Oe, and (ii) the contribution from grain boundaries, which exhibit a high magnetoresistance in weak magnetic fields [4–9]. Experimental investigations of magnetoresistive effects in these materials [5–29] have made it possible to propose a number of mechanisms of dissipation: creep and flux flow [30] (here, the motion of Josephson vortices is considered instead of classical Abrikosov vortices [1, 27]); thermally activated phase slip of the superconducting order parameter [31] (which is characteristic of Josephson junctions); the model of the vortex glass [32]; pinning at grain boundaries with fractal geometry [33, 34]; etc. In most cases, the analysis of magnetore-

sistive properties have been performed using a quantitative characteristic of the pinning of vortices, namely, the pinning potential U_p, which can depend on the temperature and magnetic field [35]. The dissipation (voltage drop in the flow of transport current) can be observed when thermal fluctuations become comparable to the pinning potential. The functional dependence of the pinning potential on the magnetic field and temperature $U_p(H, T)$ is derived from experimental data on the current–voltage characteristics, temperature dependences of electrical resistance $R(T)$ in external fields, and magnetoresistance isotherms $R(H)$, and, rather often, the form of the dependence $U_p(H, T)$ gives grounds to judge the applicability of one or other model.

At the same time, it has long been known [36] that magnetoresistance isotherms $R(H)$ have a hysteresis character. Clearly, this can lead to the influence of thermal magnetic prehistory on current–voltage characteristics [37–39] and dependences $R(T)$ [19]. To date, it has been established that the hysteresis of magnetoresistance $R(H)$ of a granular HTSC is determined by the effect of magnetic moments of HTSC grains on the intergranular medium [17, 18, 40–43]. Each point of the intergranular medium is subjected to a local magnetic field, which is a superposition of the external magnetic field and the field induced by magnetic moments of the neighboring HTSC grains (see figures showing a schematic representation of the lines of the magnetic induction in a grain boundary in [17, 42]). Simplifying such a complex distribution of the lines of the magnetic induction in the intergranular medium, we can introduce a magnetic field averaged over all intergranular spaces, i.e., the "effective" magnetic field B_{eff}. In the simplest case, this effective field can be assumed to be proportional to the magnetic moment $M(H)$ of the entire sample. Then, we obtain

$$\mathbf{B}_{\text{eff}}(H) = \mathbf{H} + \alpha \times 4\pi\mathbf{M}(H).$$

The parameter α in the expression appears due to the influence of demagnetizing factors of the grains. As applied to the processes of dissipation in the intergranular medium (where the sign of the effective field does not matter), we obtain the following expression:

$$B_{\text{eff}}(H) = |H - \alpha \times 4\pi M(H)|, \qquad (1)$$

which takes into account that, at $H > 0$ and $dH/dt > 0$, the magnetic moment of HTSC grains is negative ($M < 0$). And since the magnetoresistance is a function of the effective field, i.e., $R = f(B_{\text{eff}})$, and the dependence $M(H)$ has a hysteresis, the dependence $R(H)$ also exhibits a hysteresis.

However, a quite unexpected fact is that the matching of the parameters of the hysteretic dependence $B_{\text{eff}}(H)$ with the parameters of the hysteresis $R(H)$ requires that the value of the parameter α should be significantly larger than unity [41, 42]. For example, it was shown that, for $YBa_2Cu_3O_7$, $\alpha \approx 12$ [42]. This can be considered a manifestation of the compression of the magnetic flux in the intergranular medium. As a consequence, the effective magnetic field can be an order of magnitude higher than the value of H in the range of weak fields. This inference can lead to a serious correction to the form of the field and temperature dependences of the pinning potential $U_p(H, T)$, which are obtained from the magnetoresistive data. Indeed, since $\alpha \gg 1$, the second term of expression (1) in the low-field region is dominant, and the effective field in the intergranular medium significantly exceeds the external field [41, 42].

In our previous study [19], we showed and explained qualitatively the difference in the dependences $R(T)$ measured during cooling in a magnetic field (field cooling (FC) mode) and during cooling without a field (zero field cooling (ZFC) mode). It turned out that, for yttrium HTSC in external magnetic fields higher than ~ 5 kOe, there is no difference between the results of measurements in these modes; i.e., the second term of expression (1) does not make a significant contribution to the effective field in the intergranular medium. In the present work, at a specific temperature ($T = 77.4$ K), the magnetic prehistory of the sample was purposefully predetermined so that, at different values of the external magnetic field, the effective field in the intergranular medium would be identical. Then, in addition to measurements of the dependences $R(T)$ at a prescribed magnetic prehistory, we investigated the dependences $M(T)$, which allowed us to analyze the temperature evolution of the effective field in the intergranular medium to the critical temperature.

2. SAMPLE PREPARATION AND EXPERIMENTAL TECHNIQUE

The $YBa_2Cu_3O_7$ sample was prepared according to the standard solid-phase synthesis technology. The X-ray diffraction analysis revealed the presence of reflections only from the 1–2–3 structure. The sample had typical (for polycrystalline yttrium HTSC) values of the electrical resistance (~1 mΩ cm at 100 K, ~1.8 mΩ cm at 300 K) and critical current density (~50 A/cm^2 at 77.4 K). The density of the sample was ~85% of the theoretical value.

The magnetic and transport measurements were performed on the same sample ~1 × 1 × 8 mm in size. The dependences of the magnetoresistance $R(H) = U(H)/I$ (where U is the voltage drop and I is the transport current), temperature dependences of the electrical resistance $R(T)$, and current–voltage characteristics were measured by the standard four-point probe method. During measurements of the dependences $R(H)$ at a current $I = 150$ mA and the current–voltage characteristics up to the values of 350 mA, the sample was placed in a liquid-nitrogen medium, which made it possible to avoid self-heating effects (this was indi-

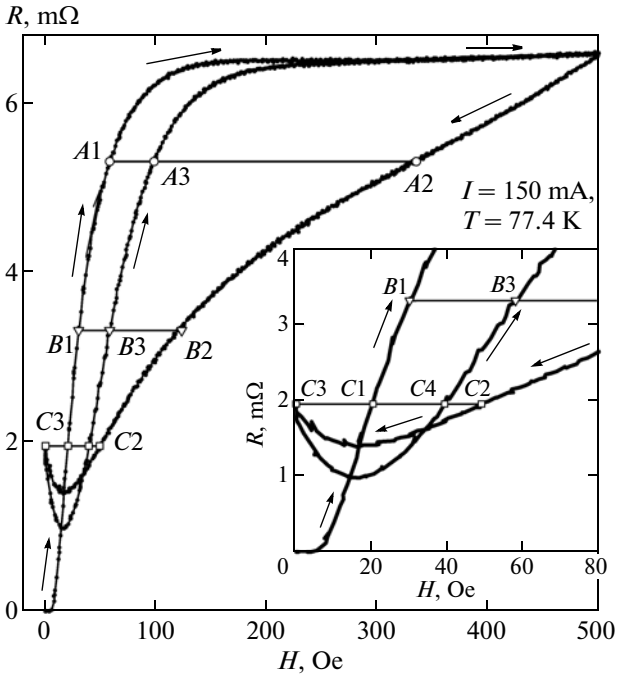

Fig. 1. Hysteretic dependence of the magnetoresistance $R(H)$ of the studied granular HTSC $YBa_2Cu_3O_7$ at T = 77.4 K. Arrows indicate the direction of variation in the external magnetic field H. A group of points ($A1$–$A3$, $B1$–$B3$, $C1$–$C4$) at R = const (horizontal lines) correspond to the magnetic prehistory for experimental data on the current–voltage characteristics and dependences $M(T)$ and $R(T)$. The external magnetic fields for the points $A1$–$A3$, $B1$–$B3$, and $C1$–$C4$ are presented in the table. The inset shows in more detail the dependence $R(H)$ in the magnetic field range up to 80 Oe.

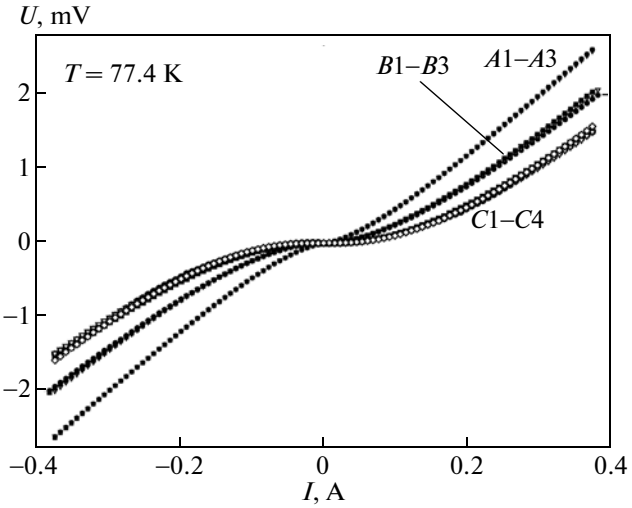

Fig. 2. Current–voltage characteristics of the studied granular HTSC $YBa_2Cu_3O_7$ at T = 77.4 K and the magnetic prehistory corresponding to the points $A1$–$A3$, $B1$–$B3$, and $C1$–$C4$ in Fig. 1.

cated by the coincidence of the forward and reverse current–voltage characteristics). The magnetic measurements were carried out on a sample-vibrating magnetometer [44]. The magnetic data are given in gauss, obtained taking into account the weight and density of the sample.

The current–voltage characteristics and temperature dependences $R(T)$ and $M(T)$ were measured for a prescribed magnetic prehistory. For this purpose, the sample was cooled in a zero external magnetic field to the liquid-nitrogen temperature. Then, the external magnetic field was generated by a copper coil solenoid at a rate of ~2 Oe/s in such a way as to achieve particular values, which were chosen both in the increasing magnetic field (H_{inc} at $dH/dt > 0$) and after the application of the field H_{max} = 500 Oe in the decreasing field (H_{dec} at $dH/dt < 0$).

3. RESULTS AND DISCUSSION

3.1. Magnetoresistance and Magnetization Hystereses and Evaluation of the Degree of Compression of a Magnetic Flux in the Intergranular Medium

The hysteretic dependence of the magnetoresistance $R(H)$ of the studied sample is shown in Fig. 1. The inset to Fig. 1 shows in more detail this dependence in the range of weak magnetic fields. In these measurements, the external magnetic field was increased to the value H_{max} = 500 Oe, then was decreased to zero, and then was increased again to the value H_{max} (denoted in this case as $H = H_{inc2}$). Under the above conditions, the dependence $R(H)$ corresponds to the sequence $H_{inc} = 0$ (here, $R = 0$) $\longrightarrow$ $C1 \longrightarrow B1 \longrightarrow A1 \longrightarrow H_{max}$ = 500 Oe $\longrightarrow A2 \longrightarrow B2 \longrightarrow C2 \longrightarrow C3$ (here, $H_{dec} = 0$) $\longrightarrow C4 \longrightarrow B3 \longrightarrow A3 \longrightarrow H_{max}$ = 500 Oe. It should be noted that, for $H_{inc2} \approx 300$ Oe, the dependence $R(H_{inc2})$ coincides with the initial course of magnetoresistance, i.e., with the dependence $R(H_{inc})$. Further, during the cycling of the external magnetic field up to H_{max} = 500 Oe and to $H_{dec} = 0$, the dependence $R(H)$ corresponds to the sequence $A2 \longrightarrow B2 \longrightarrow C2 \longrightarrow C3 \longrightarrow C4 \longrightarrow B3 \longrightarrow A3 \longrightarrow A2$.

The group of points ($A1$–$A3$, $B1$–$B3$, $C1$–$C4$) indicated in Fig. 1 are "sections" of the dependence $R(H)$ under the condition R = const. The values of the external magnetic field and magnetic prehistories for these selected points are presented in the table. The equality of the resistances for points of one group ($A1$–$A3$), ($B1$–$B3$), and ($C1$–$C4$) is confirmed by measurements of the current–voltage characteristics over a wide range of variation in the transport current (Fig. 2). It can be concluded that, within the limits of experimental error, the current–voltage characteristics are identical for the chosen measurement conditions corresponding to groups of points ($A1$–$A3$), ($B1$–$B3$), and ($C1$–$C4$).

The equality of the resistances of the sample for different magnetic prehistories (for example, for the branches H_{inc}, H_{dec}, and H_{inc2} of the hysteretic dependence $R(H)$) can be considered as the equality of the effective fields in the intergranular medium in different magnetic states. Let us estimate the value of α from expression (1) for our sample. For this purpose, it is expedient to consider not the parameter $\Delta R = R(H_{inc}) - R(H_{dec})$ (the "height" of the hysteretic dependence $R(H)$), because it depends on the transport current I, but the current-independent parameter, i.e., the width of the hysteresis $\Delta H = H_{dec} - H_{inc}$ [17, 18]. This parameter is determined under the condition $R = \text{const}$. For the magnetic field hysteresis width ΔH, from formula (1), we obtain the following expression [17, 18]:

$$\Delta H = H_{dec} - H_{inc} = \alpha \times 4\pi(M(H_{inc}) - M(H_{dec})). \quad (2)$$

In this expression, to a first approximation, the parameter α is assumed to be independent of the external field. The hysteretic dependence of the magnetic moment $M(H)$ measured under conditions similar to those used for the dependence $R(H)$ (Fig. 1) is shown in Fig. 3. In this dependence, we also specified a group of points $A1$–$A3$, $B1$–$B3$, and $C1$–$C4$, which correspond to the condition $R = \text{const}$ for the dependence $R(H)$. By comparing data on the magnetic field hysteresis width ΔH, which were obtained from the experimental dependence $R(H)$ and from the dependence $B_{eff}(H)$ (found according to expression (1) using data on the dependence $M(H)$ in Fig. 3), we established that, over a wide range of variation in the external magnetic field, these data are in good agreement for the parameter $\alpha \sim 11.8$. Such a mapping procedure was described in detail in [42] by using the example of high-density $YBa_2Cu_3O_7$ (95% of the theoretical density).

3.2. Temperature Evolution of the Magnetic Moment $M(T)$ and Effective Magnetic Field $B_{eff}(T)$ in the Intergranular Medium

The measurements of the temperature dependences of the magnetic moment $M(T)$ were performed for a predetermined magnetic prehistory. This prehistory was specified at $T = 77.4$ K and corresponded to the points $A1$–$A3$, $B1$–$B3$, and $C1$–$C4$ in Figs. 1 and 3 (see also table). In what follows, the dependences $M(T)$ (and also the dependences $B_{eff}(T)$ and $R(T)$) will be designated as corresponding to a particular magnetic prehistory (for example, $A1$).

The dependences $M(T)$ are shown in Fig. 4. Let us make a few comments regarding the form of the dependences $M(T)$. According to the generally accepted ideas (the Bean model or its modifications), the magnetic moment of the sample is formed by different contributions, for example, the contribution from Meissner currents (diamagnetism) and the contribution from the trapped magnetic flux (Abrikosov vortices giving a magnetic moment $M > 0$ for $H > 0$). The distribution of the trapped magnetic flux varies depending on the conditions. For example, at $H =$

Designations of the characteristic points $A1$–$A3$, $B1$–$B3$, and $C1$–$C4$ in the dependences $R(H)$ and $M(H)$ (Figs. 1, 3) and the external magnetic fields H corresponding to these points

Point	Field
$C1$	$H_{inc} = 20$ Oe
$C2$	$H_{dec} = 49$ Oe*
$C3$	$H_{dec} = 0$ Oe*
$C4$	$H_{inc2} = 39$ Oe**
$B1$	$H_{inc} = 30$ Oe
$B2$	$H_{dec} = 123$ Oe*
$B3$	$H_{inc2} = 58$ Oe**
$A1$	$H_{inc} = 58$ Oe
$A2$	$H_{dec} = 335$ Oe*
$A3$	$H_{inc2} = 98$ Oe**

Note: H_{inc} and H_{dec} are the increasing and decreasing external magnetic fields. The asterisks correspond to different magnetic prehistories at $T = 77.4$ K: * after the application of the maximum magnetic field of 500 Oe; ** after the increase in the magnetic field to 500 Oe and further decrease to zero. For the given magnetic history, the dependences obtained are as follows: $M(T)$ (Fig. 4), $B_{eff}(T)$ (Fig. 5) and $R(T)$ (Figs. 6–9).

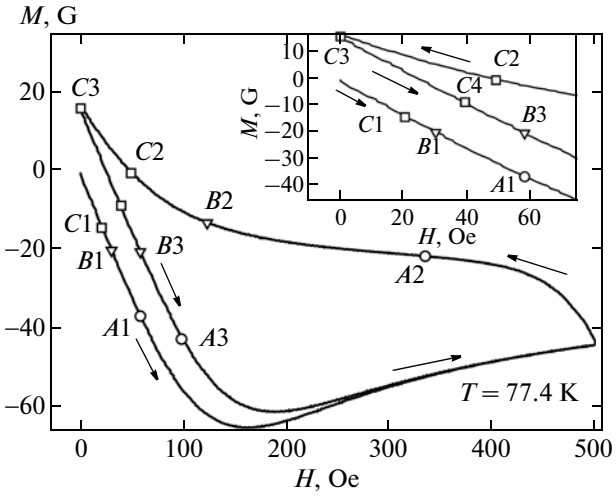

Fig. 3. Hysteretic dependence of the magnetic moment $M(H)$ of granular $YBa_2Cu_3O_7$ at $T = 77.4$ K. Arrows indicate the direction of variation in the external magnetic field H. Points $A1$–$A3$, $B1$–$B3$, and $C1$–$C4$ in the dependence $M(H)$ correspond to the analogous points in Fig. 1. The inset shows in more detail the dependence $M(H)$ in the magnetic field range up to 80 Oe.

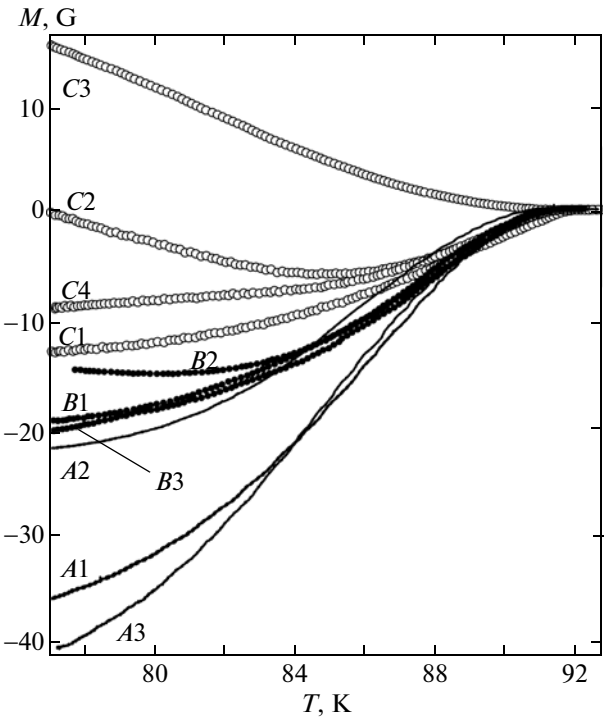

Fig. 4. Dependences $M(T)$ for different magnetic prehistories corresponding to the points $A1$–$A3$, $B1$–$B3$, and $C1$–$C4$ in Fig. 1.

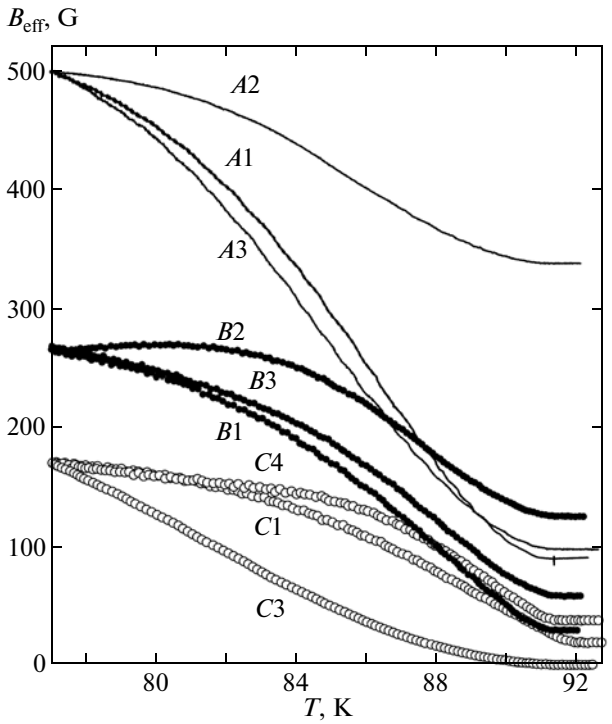

Fig. 5. Temperature evolution of the effective magnetic field in the intergranular medium $B_{eff}(T)$ obtained according to expression (1) using data on the dependence $M(T)$ shown in Fig. 4 and according to the condition $B_{eff}(T = 77.4\ \text{K}) = \text{const}$ at $R = \text{const}$ (Fig. 1) (see Subsection 3.2). Designations $A1$–$A3$, $B1$–$B3$, and $C1$–$C4$ correspond to the magnetic prehistories in Figs. 1, 3, and table.

H_{dec}, the magnetic flux is redistributed toward the center of the superconductor. In the case of a granular HTSC, these processes occur in the HTSC grains and the response from the intergranular medium in the used temperature range and in magnetic fields exceeding the Earth's field is negligibly small. Therefore, positive values of the magnetization in Fig. 4 correspond to the influence of the trapped magnetic flux inside the HTSC grains. The contributions from the Meissner currents and from the trapped magnetic flux differently depend on the temperature. This circumstance can lead to a nonmonotonic dependence $M(T)$, which is seen in the example of the dependence $M(T)$ for prehistory $C2$ (Fig. 4). For this dependence, the total magnetic moment at $T = 77.4$ K is close to zero, which means an approximate equality of the contributions corresponding to the Meissner currents and the trapped magnetic flux. However, at higher temperatures, the contribution from the trapped magnetic flux decreases more rapidly (it can be compared with the dependence $M(T)$ for prehistory $C3$, where the external field is zero), which leads to the appearance of a minimum in the dependence $M(T)$.

Using the dependences $M(T)$ (Fig. 4) and expression (1), we constructed the temperature dependences of the effective field in the intergranular medium $B_{eff}(T)$, which are shown in Fig. 5. In the construction of these dependences, the value of B_{eff} at a temperature $T = 77.4$ K was assumed to be identical for types of prehistories in which $R = \text{const}$ (Figs. 1, 2). For example, the values of B_{eff} (77.4 K) are identical for prehistories $A1$–$A3$, etc. However, it was also assumed that the value of α in expression (1) cannot be significantly different from the value $\alpha = 11.8$ obtained above (see Subsection 3.1) when comparing the values of ΔH. It turned out that the spread in values of the parameter α for different magnetic prehistories was approximately 10% relative to $\alpha = 11.8$ (for example, $\alpha = 11.8$ for $B1$, $\alpha = 9.3$ for $B2$, and $\alpha = 10.1$ for $B3$).[1] As can be seen from Fig. 5, the magnetic fields $B_{eff}(T)$ corresponding to the "sections" of the dependences $R(H)$ in Fig. 1 have identical values at $T = 77.4$ K and exceed several times the external field generated by the solenoid. An increase in the temperature leads to a noticeable decrease in the effective field in the intergranular medium to the corresponding value of the external field at $T = T_c \approx 91.5$ K.

[1] For prehistory $C2$, the value of $M(T = 77.4\ \text{K})$ is close to zero, and the relationship between M and B_{eff} is more complex than expression (1).

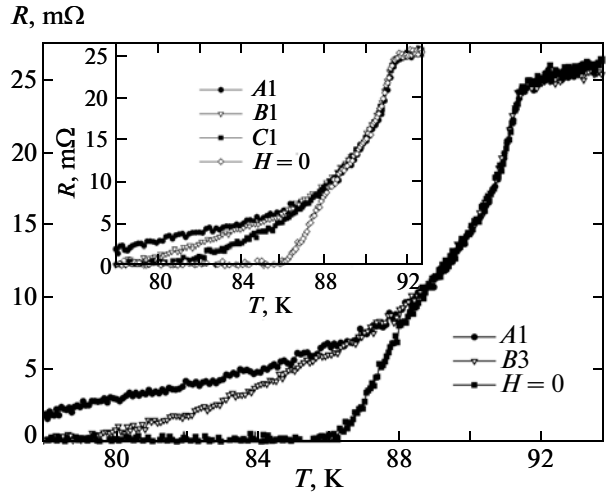

Fig. 6. Dependences $R(T)$ in external magnetic fields for different magnetic prehistories. Designations $A1$, $B1$, $C1$, and $B3$ in the main figure and inset correspond to those in Figs. 1, 3, and table.

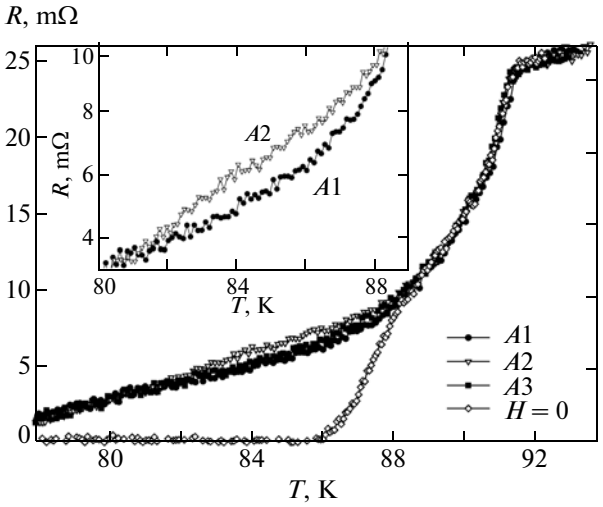

Fig. 7. Dependences $R(T)$ for different magnetic prehistories corresponding to the condition R = const in Fig. 1, the upper "section" (designations are given in the table). The inset on an enlarged scale shows of the region in which the dependences $R(T)$ for prehistories $A1$ and $A2$ diverge.

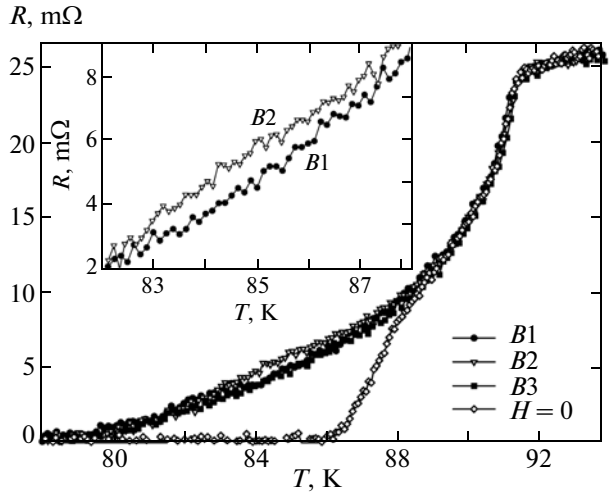

Fig. 8. Dependences $R(T)$ for different magnetic prehistories corresponding to the condition R = const in Fig. 1; points $B1$, $B2$, and $B3$ (designations are given in the table). The inset shows a fragment in which the dependences $R(T)$ for prehistories $B1$ and $B2$ diverge.

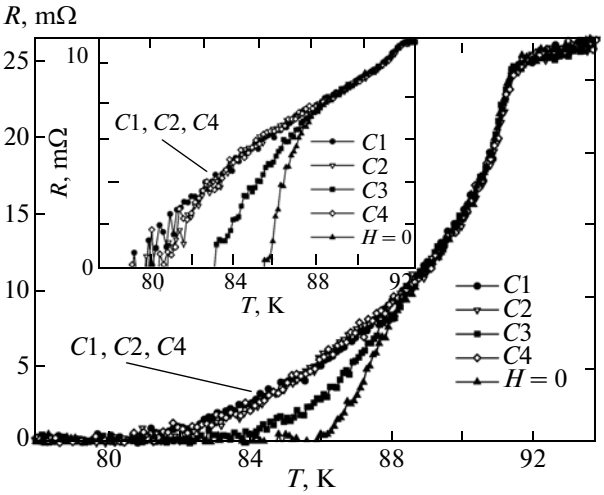

Fig. 9. Dependences $R(T)$ for different magnetic prehistories corresponding to the condition R = const in Fig. 1, the lower "section" (designations are given in the table). The inset shows the same fragment on a semi-logarithmic scale.

3.3. Temperature Dependences R(T) in an External Magnetic Field and Correlation with the Behavior of $B_{eff}(T)$

Now, we turn to the discussion of the influence of the temperature dependence of the effective magnetic field in the intergranular medium on the resistive phase transition in a granular HTSC. Under the conditions identical to those used to measure the dependences $M(T)$ (and to those used to construct the dependences $B_{\text{eff}}(T)$ in Fig. 5), we measured the dependences $R(T)$. As was noted in the Introduction, the resistive transition of a granular HTSC in an external magnetic field reflects the contributions from grains and grain boundaries. The subsystem of HTSC grains is characterized by a sharp drop in the resistance and a very weak influence of external magnetic fields up to ~10^3 Oe, while for grain boundaries, there is a broadening of the transition (the smooth part of the dependence $R(T)$) in weak magnetic fields. The above behavior is clearly seen from the experimental data

presented in Figs. 6–9 (transport current $I = 2$ mA for all data). The observed abrupt change in the electrical resistance at $T \approx 91.5$ K corresponds to the beginning of the resistive transition in the grains and coincides with the appearance of a diamagnetic signal in the dependences $M(T)$ in the zero field cooling mode (Fig. 4).

The inset to Fig. 6 shows the resistive transition of the studied sample at different external magnetic fields (including also $H = 0$) in the zero field cooling mode with the further application of a magnetic field H. It is in this way that the vast majority of measurements have been carried out for HTSC samples. The data presented in the inset to Fig. 6 demonstrate the well-known picture: a weak external magnetic field substantially decreases the temperature of the transition to a "zero resistance state" (~10^{-5} Ω in our case). For example, the value of this characteristic temperature ($R \approx 0$) varies from ~86 K at $H = 0$ to ~81 K at $H =$ 20 Oe.[2] However, Fig. 6 shows the dependences measured in the same external field of 58 Oe ($A1$ and $B3$) but with different magnetic prehistories (see table), which clearly demonstrate that the dissipation in the case of $A1$ begins to occur at a considerably lower temperature. This behavior can be explained by comparing the dependences $B_{\text{eff}}(T)$ for prehistories $A1$ and $B3$ (Fig. 5). For example, at $T = 80$ K, the value B_{eff} for prehistory $A1$ is almost two times larger than that for prehistory $B3$, and the resistance for prehistory $B3$ at $T = 80$ K only begins to increase from a "zero" value.

Figures 7–9 show the dependences $R(T)$ grouped for the magnetic prehistories in which $R =$ const at $T = 77.4$ K, i.e., for the conditions $A1$–$A3$ (Fig. 7), $B1$–$B3$ (Fig. 8), and $C1$–$C4$ (Fig. 9). Let us consider these data in more detail.

The dependences $R(T)$ for prehistories $A1$ and $A3$ (Fig. 7), within the limits of experimental error, coincide with each other despite the difference in the external magnetic fields (58 and 98 Oe, respectively). This can be easily explained by considering the temperature evolution of the effective field B_{eff} (Fig. 5) for these prehistories. Indeed, the functions $B_{\text{eff}}(T)$ for prehistories $A1$ and $A3$ differ by no more than 10%, which does not radically affect the dissipation processes. The dependence $B_{\text{eff}}(T)$ for prehistory $A2$ decreases more weakly than the aforementioned dependences $B_{\text{eff}}(T)$ for prehistories $A1$ and $A3$. This leads to the higher resistance observed in Fig. 7 in the corresponding dependence $R(T)$ for prehistory $A2$ (which is illustrated in the inset to Fig. 7).

A similar pattern is observed for the prehistory corresponding to the group of points $B1$, $B2$, and $B3$ (Fig. 8). The dependences $R(T)$ for prehistories $B1$ and $B3$ are almost identical, as well as the dependences $B_{\text{eff}}(T)$ for prehistories $B1$ and $B3$ (Fig. 5). However, the dependence $R(T)$ for prehistory $B2$ in the temperature range of 82–88 K differs significantly from the dependence $R(T)$ for prehistories $B1$ and $B3$ (inset to Fig. 8). This is associated with the fact that the effective magnetic field for prehistory $B2$ is approximately 40–60 G higher (relative to the value of ~200 G) than the effective field B_{eff} for prehistories $B1$ and $B3$ in this temperature range. It is also seen from Figs. 7 and 8 that, at $T = 78$ K, the resistances for the corresponding dependences ($A1$–$A3$ and $B1$–$B3$) coincide with each other, which agrees with the data on the current–voltage characteristics for these prehistories (Fig. 2).

The dependences $R(T)$ for prehistories $C1$, $C2$, and $C4$ (Fig. 9), within the limits of experimental error, coincide with each other, which again is confirmed by the similarity of the dependences $B_{\text{eff}}(T)$ for these conditions (see $B_{\text{eff}}(T)$ in Fig. 5 for prehistories $C1$ and $C4$). However, the dissipation for prehistory $C3$ (zero external field after the application of the field $H_{\max} =$ 500 Oe) begins at a substantially higher temperature, which is illustrated in the inset to Fig. 9 (logarithmic scale for R). At the same time, at $T = 77.4$ K, the resistance at a high transport current for prehistories $C1$, $C2$, $C3$, and $C4$ has the same values (Figs. 1, 3). This is not surprising in view of the significantly lower effective field in the intergranular medium for prehistory $C3$ beginning from the temperature of approximately 80 K.

Based on the above consideration, it can be concluded that, in measurements of the temperature dependences of the electrical resistance $R(T)$ in external magnetic fields, the temperature evolution of the effective magnetic field in the intergranular medium has a significant influence on the shape of the dependence $R(T)$. Thus, the obtained data have confirmed that, in a specified external magnetic field, grain boundaries are in an effective magnetic field which depends on the magnetic moment of the sample, and this effective magnetic field exerts a dominant influence on the processes of dissipation in the intergranular medium.

4. CONCLUSIONS

Summarizing the results obtained in the course of the performed investigations, we can conclude that the magnetic state of HTSC grains exerts a dominant influence on the processes of dissipation in the intergranular medium of granular HTSCs. The magnetic moments of the grains induce a magnetic field in the intergranular medium, which for weak external magnetic fields (up to ~10^2 Oe) can be an order of magnitude superior to the external magnetic field. This effect occurs as a result of compression of the magnetic flux in the intergranular medium [42]. Consequently, the temperature evolution of the magnetization of HTSCs in a constant external magnetic field leads to a strong

[2] The temperature at which $\langle\langle R = 0 \rangle\rangle$ also depends on the transport current: this temperature decreases with an increase in the current.

dependence of the effective magnetic field in the intergranular medium on the temperature. It is this dependence that can be a dominant factor determining the shape of the experimentally observed dependences $R(T)$. In other words, in the measurements of granular HTSCs in an external magnetic field, the actual value of the field (magnetic induction) in the intergranular medium is not constant with variations in the temperature. This fact casts doubt on numerous interpretations of the behavior of the dependences $R(T)$ and current–voltage characteristics of granular HTSCs in external magnetic fields up to $\sim 10^2$–10^3 Oe, i.e., in the range of fields where the influence of magnetic moments of HTSC grains on the field in the intergranular medium is significant. For example, the dependence $R(T)$ can follow any of the models of dissipation (listed in the Introduction) for a specific temperature dependence of the pinning potential; however, in this case, the magnetic field is assumed to be constant, which is not the case. This is also true for scaling of the current–voltage characteristics at different temperatures [20–23], following from the model of the vortex glass [32], for which the effective magnetic field in the intergranular medium also varies at different temperatures.

Therefore, the understanding of mechanisms actually reflecting the real picture of dissipation in the Josephson medium of a granular HTSC in an external magnetic field (despite numerous publications since the discovery of high-temperature superconductivity) has remained an important problem which can be solved by considering the full picture of phenomena (including magnetic fields in the intergranular medium) induced by magnetic moments of HTSC grains. It should also be noted that the influence of magnetic moments of HTSC grains and the compression of a magnetic flux in the intergranular medium are apparently dominant factors that determine a significant magnetoresistive effect observed in granular HTSCs.

ACKNOWLEDGMENTS

This study was supported by the Russian Foundation for Basic Research (project no. 13-02-00358).

REFERENCES

1. E. B. Sonin, JETP Lett. **47** (8), 496 (1988).
2. J. Jung, A. K. Mohamed, S. C. Cheng, and J. P. Frank, Phys. Rev. B: Condens. Matter **42** (10), 6181 (1990).
3. B. Andrzejewski, E. Guilmeau, and Ch. Simon, Supercond. Sci. Technol. **14**, 904 (2001).
4. M. A. Dubson, S. T. Herbert, J. J. Calabrese, D. C. Harris, B. R. Patton, and J. C. Garland, Phys. Rev. Lett. **60** (11), 1061 (1988).
5. J. D. Hettinger, A. G. Swanson, J. S. Brooks, Y. Z. Huang, L. Q. Chen, and Zhong-Xian Zhao, Supercond. Sci. Technol. **1**, 349 (1989).
6. H. S. Gamchi, G. J. Russel, and K. N. R. Taylor, Phys. Rev. B: Condens. Matter **50** (17), 12950 (1994).
7. C. Gaffney, H. Petersen, and R. Bednar, Phys. Rev. B: Condens. Matter **48** (5), 3388 (1993).
8. A. C. Wright, K. Zhang, and A. Erbil, Phys. Rev. B: Condens. Matter **44** (2), 863 (1991).
9. A. C. Wright, T. K. Xia, and A. Erbil, Phys. Rev. B: Condens. Matter **45** (2), 5607 (1992).
10. C. A. M. dos Santos, M. S. da Luz, and A. J. S. Machado, Physica C (Amsterdam) **391**, 345 (2003).
11. D. Daghero, P. Mazzetti, A. Stepanesku, P. Tura, and A. Masoero, Phys. Rev. B: Condens. Matter **66**, 184514 (2002).
12. L. Urba, C. Acha, and V. Bekeris, Physica C (Amsterdam) **279**, 92 (1997).
13. M. R. Mohammadizadeh and M. Akhavan, Supercond. Sci. Technol. **16**, 234 (2003).
14. H. Shakeripour and M. Akhavan, Supercond. Sci. Technol. **14**, 234 (2001).
15. D. A. Balaev, K. A. Shaihutdinov, S. I. Popkov, D. M. Gokhfeld, and M. I. Petrov, Supercond. Sci. Technol. **17**, 175 (2004).
16. D. A. Balaev, S. I. Popkov, K. A. Shaikhutdinov, and M. I. Petrov, Phys. Solid State **48** (5), 826 (2006).
17. D. A. Balaev, D. M. Gokhfeld, A. A. Dubrovskii, S. I. Popkov, K. A. Shaikhutdinov, and M. I. Petrov, JETP **105** (6), 1174 (2007).
18. D. A. Balaev, A. A. Dubrovskii, K. A. Shaikhutdinov, S. I. Popkov, D. M. Gokhfeld, Yu. S. Gokhfeld, and M. I. Petrov, JETP **108** (2), 241 (2009).
19. D. A. Balaev, A. A. Bykov, S. V. Semenov, S. I. Popkov, A. A. Dubrovskii, K. A. Shaikhutdinov, and M. I. Petrov, Phys. Solid State **53** (5), 922 (2011).
20. T. K. Worthington, E. Olsson, T. M. Nichols, T. M. Shaw, and D. R. Clarke, Phys. Rev. B: Condens. Matter **43**, 10538 (1991).
21. W. M. Tieran, R. Joshi, and R. B. Hallock, Phys. Rev. B: Condens. Matter **48**, 3423 (1993).
22. Y. Zhao, X. B. Zuge, J. M. Xu, and L. Cao, Phys. Rev. B: Condens. Matter **49**, 6985 (1994).
23. R. J. Joshi, R. B. Hallock, and J. A. Taylor, Phys. Rev. B: Condens. Matter **55**, 9107 (1997).
24. R. J. Soulen, T. L. Francavilla, W. W. Fuller-Mora, M. M. Miller, C. H. Joshi, W. L. Carter, A. J. Rodenbush, M. D. Manlief, and D. Aized, Phys. Rev. B: Condens. Matter **50**, 478 (1994).
25. D. H. Liebenberg, R. J. Soulen, T. L. Francavilla, W. W. Fuller-Mora, P. C. McIntyre, and M. J. Cima, Phys. Rev. B: Condens. Matter **51**, 11838 (1995).
26. R. J. Soulen, T. L. Francavilla, A. R. Drews, L. Toth, M. S. Osofsly, W. L. Lechter, and E. F. Skelton, Phys. Rev. B: Condens. Matter **51**, 1393 (1995).
27. N. D. Kuz'michev, Phys. Solid State **43** (11), 2012 (2001).
28. M. A. Vasyutin, Tech. Phys. Lett. **37** (8), 743 (2011).
29. K. Yu. Terent'ev, D. M. Gokhfel'd, S. I. Popkov, K. A. Shaikhutdinov, and M. I. Petrov, Phys. Solid State **53** (12), 2409 (2011).
30. P. W. Anderson, Phys. Rev. Lett. **9**, 309 (1962).

31. V. Ambegaokar and B. I. Halperin, Phys. Rev. Lett. **22**, 1364 (1969).
32. M. P. A. Fisher, Phys. Rev. Lett. **62**, 1415 (1989).
33. Yu. I. Kuzmin, Phys. Rev. B: Condens. Matter **64**, 094519 (2001).
34. Yu. I. Kuzmin, Phys. Solid State **43** (7), 1199 (2001).
35. G. Blatter, M. V. Feigel'man, V. B. Geshkenbein, A. I. Larkin, and V. M. Vinokur, Rev. Mod. Phys. **66** (4), 1125 (1994).
36. Y. J. Quian, Z. M. Tang, K. Y. Chen, B. Zhou, J. W. Qui, B. C. Miao, and Y. M. Cai, Phys. Rev. B: Condens. Matter **39**, 4701 (1989).
37. M. T. Gonzalez, S. R. Curras, J. Maza, and F. Vidal, Phys. Rev. B: Condens. Matter **63**, 224511 (2001).
38. V. V. Derevyanko, T. V. Sukhareva, and V. A. Finkel', Phys. Solid State **48** (8), 1455 (2006).
39. T. V. Sukhareva and V. A. Finkel, Phys. Solid State **53** (5), 914 (2011).
40. T. V. Sukhareva and V. A. Finkel, Phys. Solid State **50** (6), 1001 (2008).
41. K. A. Shaikhutdinov, D. A. Balaev, S. I. Popkov, and M. I. Petrov, Phys. Solid State **51** (6), 1105 (2009).
42. D. A. Balaev, S. I. Popkov, E. I. Sabitova, S. V. Semenov, K. A. Shaykhutdinov, A. V. Shabanov, and M. I. Petrov, J. Appl. Phys. **110**, 093918 (2011).
43. D. A. Balaev, A. A. Dubrovskii, S. I. Popkov, D. M. Gokhfeld, S. V. Semenov, K. A. Shaikhutdinov, and M. I. Petrov, Phys. Solid State **54** (11), 2155 (2012).
44. A. D. Balaev, Yu. V. Boyarshinov, M. M. Karpenko, and B. P. Khrustalev, Prib. Tekh. Eksp., No. 3, 167 (1985).

Translated by O. Borovik-Romanova